Supplemental Information

Title: Distinct brain regional proteome changes in the rTg-DI rat model of cerebral amyloid angiopathy
Authors: Joseph M. Schrader, Feng Xu, and William E. Van Nostrand

Supplemental Methods

Immunohistochemical analyses

Paraformaldehdye-fixed brain sections were cut in the sagittal plane at 10 μm thickness using a microtome (Leica, Buffalo Grove, IL), placed on slides and then rehydrated by immersing in xylene with decreasing concentrations of ethanol. Antigen retrieval was conducted via 5 min incubation with proteinase K (IB05406, IBI Scientific, Peosta, IA) (0.2 mg/ml) at 22^{o} C. Tissue sections were then blocked in Superblock blocking buffer (cat. #37518, ThermoFisher, Franklin, MA) containing 0.3% Triton X-100 at room temperature for 30 min and incubated with individual primary antibodies at the following dilutions overnight: rabbit polyclonal antibody to collagen IV to detect cerebral blood vessels (1:250, SD2365885, Invitrogen, Waltham, MA), goat polyclonal antibodies to glial fibrillary acidic protein (GFAP, 1:250, RRID: AB_880202, Abcam, Cambridge,

MA) or ionized calcium-binding adapter molecule 1 (Iba-1, 1:250, RRID: AB_521594, Novus, Centennial, CO) for detecting astrocytes and microglia, respectively or rabbit polyclonal antibody to Anax3 (PA5082483, Invitrogen, Waltham, MA). Primary antibodies were detected with Alexa Fluorescent 594 (RRID: AB_141359, Molecular Probes, Leiden, Netherlands) or 488 (RRID: AB_2535792, Invitrogen, Waltham, MA) -conjugated secondary antibodies (1:1000). Deposited fibrillar amyloid was detected with either thioflavin S (123H0598, Sigma-Aldrich, St. Louis, MO) or Amylo-Glo (TR-300-AG, Biosensis Inc., Thebarton, South Australia), as described by the manufacturer. Calcium staining was performed via the Von Kossa method as previously described (Rungby *et al*. 1993; Davis *et al.* 2018). Immunohistological images were captured on a KEYENCE BZ-X710 fluorescence microscope and analyzed with BZ-X Analyzer software (Version 1.3.1.1, 2013, Keyence, Itasca, IL).

Stereological counting of astrocytes and microglia

The numbers of astrocytes and microglia in the cortex, hippocampus and thalamus in rTg-DI rats and wild-type rats at 12 months of age were determined using stereological principles (Long *et al*. 1998). The total numbers of microglia and astrocytes were estimated using the Stereologer software system (Systems Planning and Analysis). Every tenth section cut at 50 μm was selected and generated 10-15 sections per reference space in a systematic-random manner. Immuno-positive cells were counted using the optical fractionator method with the dissector principle and unbiased counting rules (Long *et al*. 1998). Criteria for counting cells required that cell bodies exhibited positive GFAP or Iba-1 immunostaining, for astrocytes or microglia respectively as previously described (Zhu *et al*. 2020).

Quantitative immunoblotting

20 sagittal sections (25 μm thick) of fresh frozen 12 M whole rat brain were lysed in RIPA buffer via sonication (12 × 1 sec bursts) on ice, followed by 1 h incubation on ice, and samples were normalized to equal total protein concentrations. Sufficient 2× SDS sample buffer (2% (w/v) SDS, 0.01% (w/v) bromphenol blue, 20 mM DTT, 50 mM Tris-HCl, pH6.8) was added to each sample for final concentration of 1×. Proteins were resolved via SDS-PAGE and transferred to polyvinylidene difluoride (PVDF) membrane (Imobilon-FL, EMD Millipore, Billerica, MA). Gfap was detected by probing with an anti-GFAP rabbit polyclonal antibody (RRID: AB_10013382, Dako, Glostrup, Denmark), Apoe was detected by probing with an anti-Apoe rabbit monoclonal antibody (RRID: AB_2832971, Abcam, Cambridge, MA), Anxa3 was detected by probing with an anti-Anxa3 rabbit polyclonal antibody (PA5082483, Invitrogen, Waltham, MA), Aqp4 was detected by probing with an anti-Aqp4 rabbit polyclonal antibody RRID: AB_1006038, Novus Biologicals, Littleton, CO), MBP was detected by probing with a previously validated affinity-purified goat polyclonal antibody, and β-actin was detected by probing with a mouse monoclonal anti-β-actin (Sigma, A5441). All primary antibody dilutions were 1:5000, in 3% (w/v) BSA in PBS. Blots were then probed with appropriate horseradish peroxidase (HRP) - conjugated or fluorescent secondary antibodies (IRDye®, RRID: AB_10953628, LI-COR, Lincoln, NE). HRP-catalyzed chemiluminescent signal was revealed using SuperSignal™West Femto Maximum Sensitivity Substrate (cat# 34096, ThermoFisher, Franklin, MA,) and both chemiluminescent and fluorescent signals were detected and quantified using an Odyssey Fc imager (LI-COR, Lincoln, NE).

References

Davis J., Xu F., Hatfield J., Lee H., Hoos M. D., Popescu D., Crooks E., et al. (2018) A novel transgenic rat model of robust cerebral microvascular amyloid with prominent vasculopathy. *Am. J. Pathol.* **188**, 2877–2889.

Long J.M., Kalehua A.N., Muth N.J., Hengemihle J.M., Jucker M., Calhoun M.E., Ingram D.K., Mouton P.R.: (1998) Stereological estimation of total microglia number in mouse hippocampus. *J. Neurosci. Methods* **84,** 101-108.

Rungby J., Kassem M., Fink Eriksen E., Danscher G. (1993) The von Kossa reaction for calcium deposits: silver lactate staining increases sensitivity and reduces background. *Histochem J.* **25**, 446–451.

Zhu X., Hatfield J., Sullivan J. K., Xu F., Van Nostrand W. E. (2020) Robust neuroinflammation and perivascular pathology in rTg-DI rats, a novel model of microvascular cerebral amyloid angiopathy. *J. Neuroinflammation* **17**.

Supplemental Fig. S1

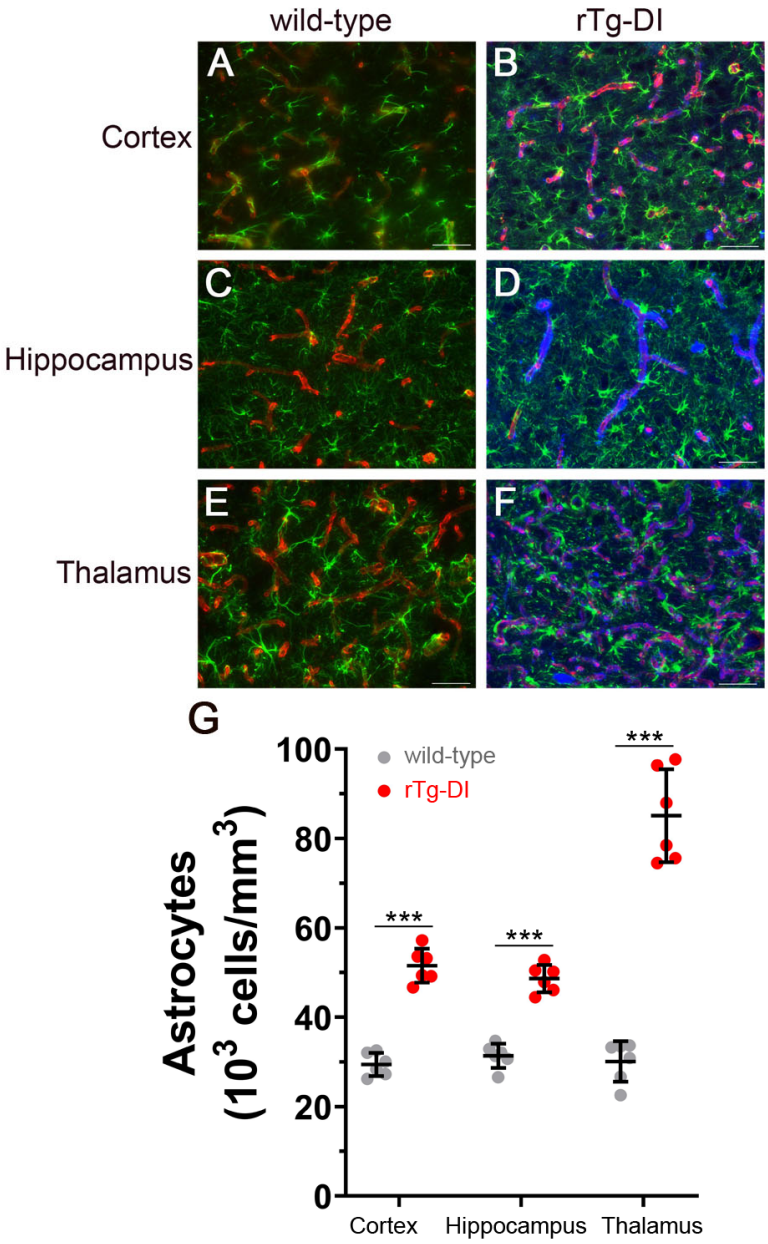

SI Fig. S1. Increased perivascular astrocytes in rTg-DI rats. Brain sections from 12 M wild-type rats (**A,C,E**) and rTg-DI rats (**B,D,F**) were labeled with Amylo-Glo to detect microvascular fibrillar amyloid (blue), goat polyclonal antibody to collagen IV to detect cerebral microvessels (red), and rabbit polyclonal antibody to GFAP to detect astrocytes (green). Scale bars = 50 μm.

(**G**) Quantitation of astrocyte numbers from rTg-DI rats (red circles) and wild-type rats (gray circles) in different brain regions at 12 months of age. Data points show the results from each rat and the group mean ± SD of n=6 rTg-DI rats and n=6 WT rats. Compared to wild-type rats the astrocyte numbers were markedly elevated in rTg-DI rats at 12 months of age in each measured brain regions. *** $P < 0.001$.

Supplemental Fig. S2

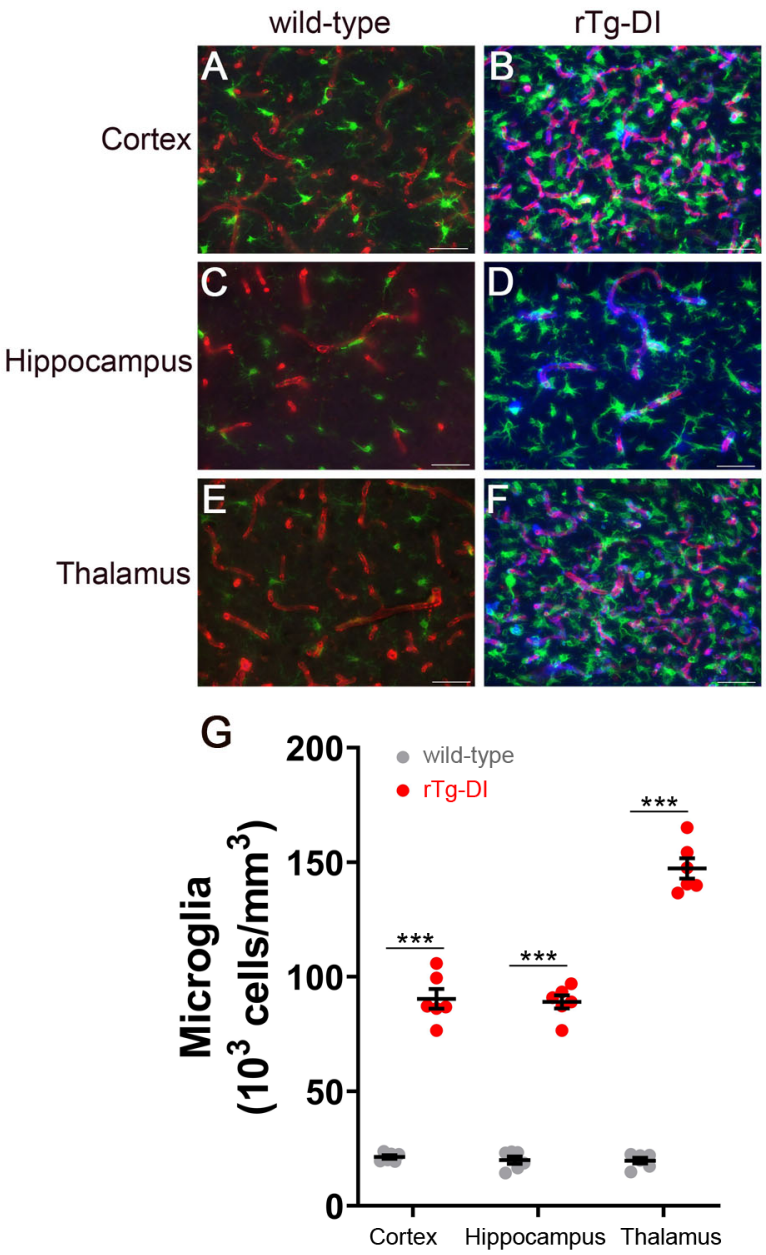

SI Fig. S2. Elevated perivascular microglia in rTg-DI rats. Brain sections from 12 M wild-type rats (**A,C,E**) and rTg-DI rats (**B,D,F**) were labeled with Amylo-Glo to detect microvascular fibrillar amyloid (blue), rabbit polyclonal antibody to collagen IV to detect cerebral microvessels (red), and goat polyclonal antibody Iba-1 to identify microglia (green). Scale bars = 50 µm. (**G**)

Quantitation of microglia numbers from rTg-DI rats (red circles) and wild-type rats (gray circles) in different brain regions at 12 months of age. Data points show the results from each rat and the group mean ± SD of n=6 rTg-DI rats and n=6 WT rats. Compared to wild-type rats the microglia numbers were markedly elevated in rTg-DI rats at 12 months of age in each measured brain regions. *** $P < 0.001$.

Supplemental Fig. S3

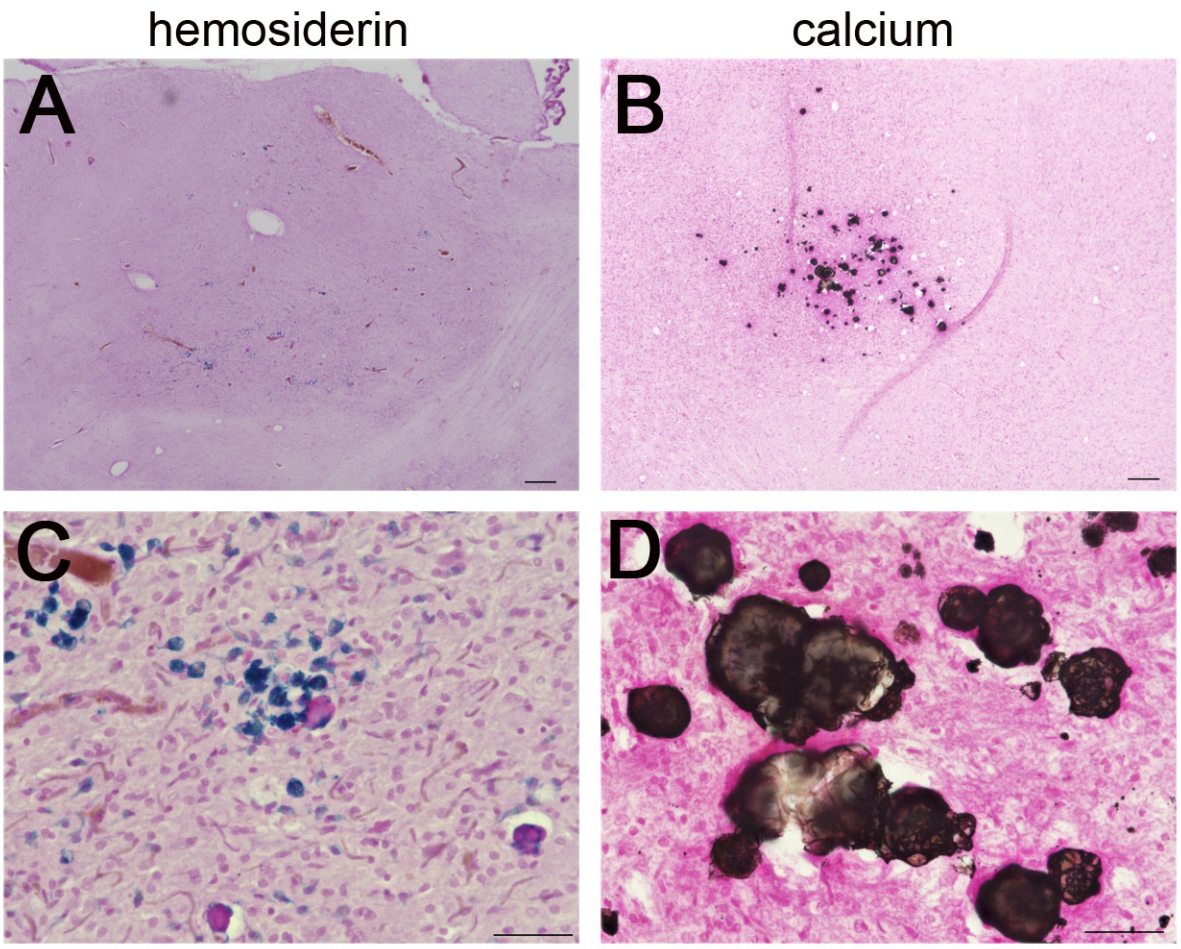

SI Fig. S3. Prominent thalamic cerebral microbleeds and occluded microvessels in rTg-DI Rats. Brain sections from the present cohort of 12 M rTg-DI rats were stained for hemosiderin to identify thalamic microbleeds (blue) (**A,C**) or stained for calcium using the von Kossa technique to identify thalamic occluded microvessels (black) (**B,D**). Scale bars = 200 µm (**A,B**) and 50 µm (**C,D**). Representative images show that consistent cerebral microbleeds and calcified, occluded vessels are observed localized in the thalamus.

Supplemental Fig. S4

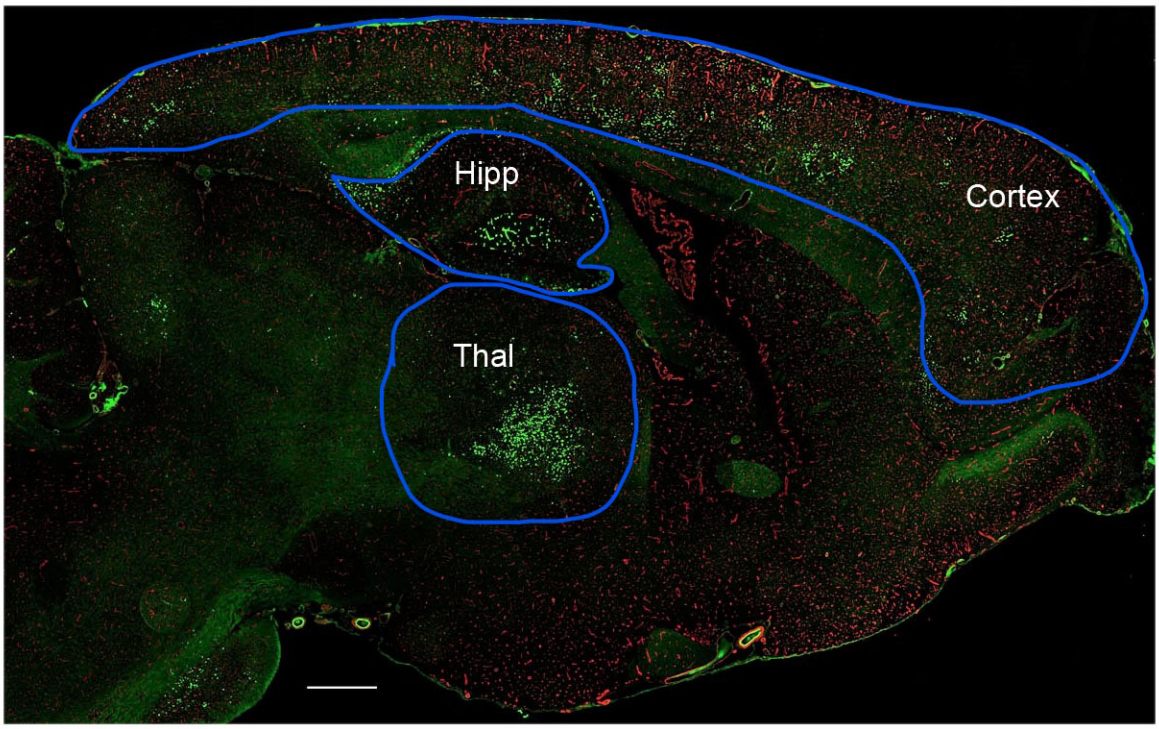

SI Fig. 4. Collection of distinct brain regions of rTg-DI rats for proteomic analysis. The cortex, hippocampus and thalamus were collected from fresh frozen rTg-DI and WT rat brain tissue sections using laser capture microdissection as described in 'Materials and Methods'. The three regions that were collected – Cortex, Hippocampus and Thalamus – are outlined in blue. Scale bar = 1mm.

Supplemental Fig. S5

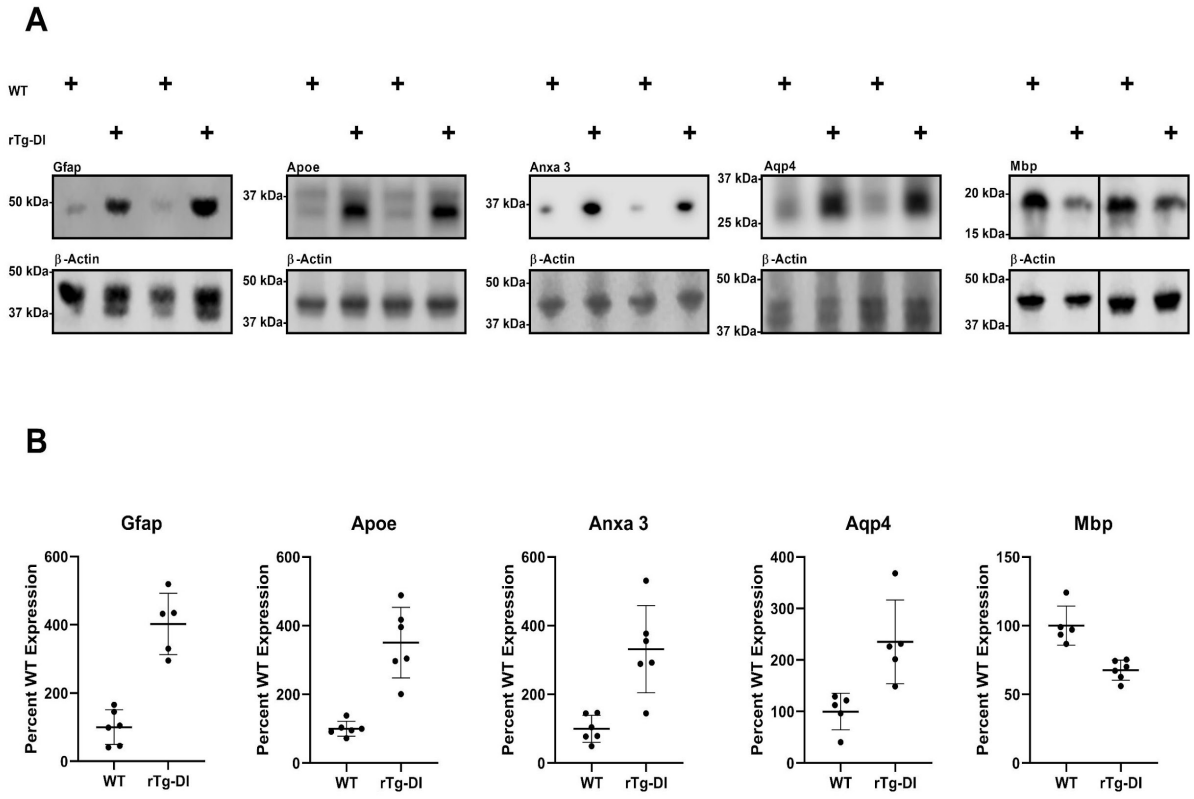

SI Fig. S5 SWATH-MS Validation by immunoblot. A. Representative lanes from immunoblotting depict the relative whole brain expression in WT and rTg-DI rats of proteins (Gfap, Apoe, Anxa3, Aqp4 and Mbp from left to right) indicated as differentially expressed in rTg-DI rats by SWATH-MS. Relative signal for the proteins of interest (top) was revealed by probing with appropriate primary antibody, and subsequent HRP-conjugated or fluorescent secondary antibody. Relative β-actin signal (bottom) revealed by probing with anti-β-actin primary antibody and subsequent fluorescent secondary antibody was used for a loading control, as β-actin is not changed in rTg-DI rats. **B.** Quantification of relative whole brain expression of Gfap, Apoe, Anxa3, Aqp4 and Mbp in WT and rTg-DI rats. Levels of protein

expression visualized in (**A**) were normalized against the corresponding β-actin signal and reported as a percentage of the WT expression. All depicted proteins displayed significantly different expression in rTg-DI rats as compared to WT, with $p = 2.99 \times 10^{-5}$ for Gfap, $p = 8.22 \times 10^{-5}$ for Apoe, $p = 8.2 \times 10^{-4}$ for Anxa3, $p = 4.59 \times 10^{-3}$ for Aqp4, and $p = 4.29 \times 10^{-4}$ for Mbp (student's t test, n = 5,6). Individual values are depicted with bars representing the mean ± SD.

Supplemental Figure S6

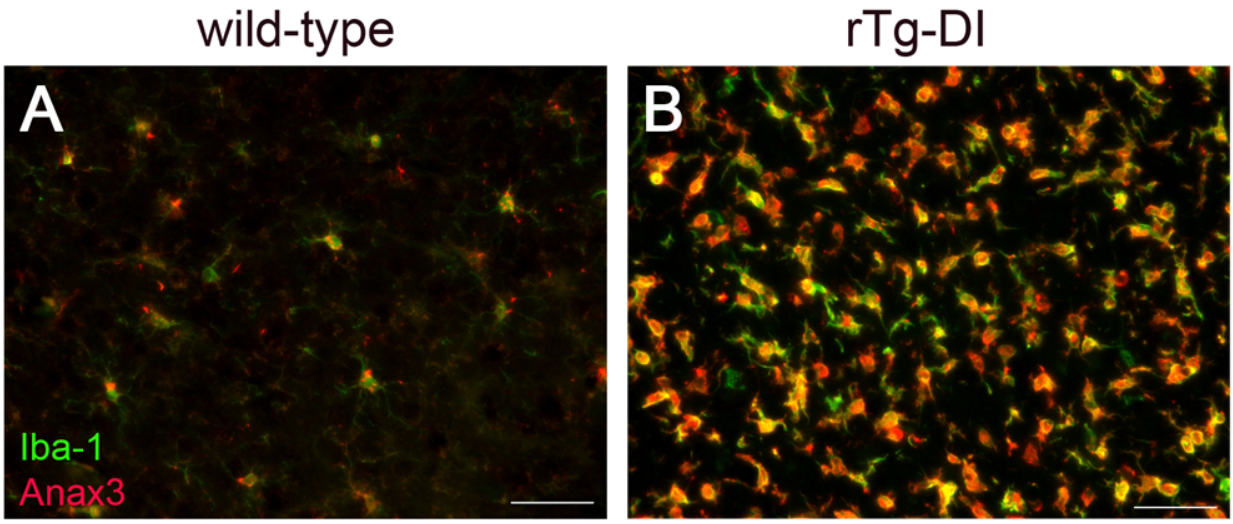

SI Fig. S6. Co-localization of Anax3 and Iba-1 labeling in microglia in rTg-DI rats. Brain sections from 12 M wild-type rats (**A**) and rTg-DI rats (**B**) were immunolabeled with a goat polyclonal antibody Iba-1 to identify microglia (green) and rabbit polyclonal antibody to Anax3 (red). The thalamic region of each rat is shown. Scale bars = 50 μm. Increased Anax3 immunoreactivity strongly co-localized with Iba-1 labeling of microglia in rTg-DI rats.